# Energy of the superallowed $\beta$ decay of $^{38}K^m$

P. D. Harty, N. S. Bowden, and P. H. Barker
*Physics Department, University of Auckland, Private Bag 92019, Auckland, New Zealand*

P. A. Amundsen
*Stavanger College, Stavanger, Norway*

(Received 31 March 1998)

The threshold energy of the $^{38}\mathrm{Ar}(p,n)^{38}K^m$ reaction has been measured using solid $^{38}$Ar targets and has been found to be 7008.52(12) keV, with a 1 V standard as reference. This is in agreement with, but more precise than, the accepted value. The average gives a $Q$ value for the $^{38}K^m$ superallowed positron decay of 6044.34(12) keV and an ft value of 3049.4(21) s. To improve this last, the discord in the measured $^{38}K^m$ halflives should be resolved. [S0556-2813(98)04308-8]

PACS number(s): 21.10.Dr, 23.40.−s, 27.30.+t

## I. INTRODUCTION

The intensities, or ft values, of the superallowed positron decays between members of $0^+$, $T=1$ isospin triplets should be identical according to the predictions of the conserved vector current (CVC) theory. In addition, a comparison with the similar intensity from muon decay enables a test to be made of the unitarity of the first row of the Cabibbo-Kobayashi-Maskawa (CKM) matrix. Thirdly, the value of $G_V$, the weak interaction vector coupling constant, which is derived from the ft values, may be compared with the value obtained from studying the decay of the neutron.

At present, nine of the nuclear positron decays have been investigated sufficiently to allow the extraction of the ft value with a precision approaching 0.1%. The experimental results were summarized in detail by Hardy *et al.* [1] and then updated subsequently [2,3]. It can be seen that the CVC prediction seems to hold good at the 0.1% level, but that the CKM unitarity referred to is problematic, and there is almost certainly disagreement with the value of $G_V$ extracted from the neutron decay results.

A particular problem for the $T=1$ nuclear decays is that the simple ft values must be modified with charge-dependent corrections, some of which are nucleus dependent and therefore sensitive to the choice of nuclear structure model used. The magnitude of these corrections is of a few tenths of a percent, and there is ongoing discussion as to the details of the calculations (see Ref. [2] or [3]). Since the nuclei range from $Z=5$ to $Z=26$, i.e., from the $1p_{3/2}$ shell to the $1f_{7/2}$ shell, it might be expected that structure-dependent errors in the correction estimates would have an impact on a CVC test, whereas problems with CKM unitarity or $G_V$ would indicate more general areas of concern, either with the superallowed ft values, or possibly with neutron decay data or the data from which the other elements of the CKM matrix are extracted.

The present work is part of an ongoing program to refine and strengthen the data base upon which the predictions deriving from the superallowed beta decays rest. In particular, we have developed a technique, HISS, such that the energy distribution of a proton beam derived from our accelerator is known very precisely, and its energy known absolutely on the scale of the ''maintained'' volt to a precision of 10 ppm or better. Recent measurements, Lin *et al.* [4], Brindhaban *et al.* [5], have given the $Q$ values of the positron decays of $^{26}Al^m$ and $^{34}$Cl by determining the $Q$ values of associated $(p,n)$ or $(p,\gamma)$ reactions.

We now report on a determination of the threshold energy of the $^{38}\mathrm{Ar}(p,n)^{38}K^m$ reaction and hence of the $Q$ value of the positron decay of $^{38}K^m$. From Ref. [1] it may be seen that this has been measured three times before, with results 6042.8(34) keV (Squier *et al.* [6], updated in Ref. [1]), 6043.7(6) keV (James *et al.* [7], updated in Ref. [1]), and 6044.6(18) keV (Burcham *et al.* [8], updated in Ref. [1]). Although these are in satisfactory agreement, with a mean 6043.76(56) keV, the error is very large, in fact the largest proportionately of all the nine decays, and it contributes significantly to the error in the ft value.

Of the three measurements cited above, each chose a different method of overcoming the twin difficulties which are inherent: the fact that $^{38}$Ar is gaseous under normal conditions of temperature and pressure, and the necessity of measuring with high precision a reaction energy of several MeV and tying that energy to an absolute scale. Burcham *et al.* [8] used a gas target with an entrance foil and compared the shifted and degraded $^{38}\mathrm{Ar}(p,n)$ yield curve around threshold with a similar one from $^{35}\mathrm{Cl}(p,n)$. James *et al.* [7] used a solid $^{38}$Ar target at low temperature and relied on the linearity of the response of their accelerator analyzing magnet to compare the $^{38}\mathrm{Ar}(p,n)^{38}K^m$ threshold energy at 7 MeV with those of $^{10}\mathrm{C}(p,n)^{10}$B at 4.88 MeV and $^{14}\mathrm{N}(p,n)^{14}$O at 6.35 MeV. Squier *et al.* [6] compared the $Q$ values of the $^{35}\mathrm{Cl}(\alpha,p)^{38}$Ar and $^{35}\mathrm{Cl}(\alpha,n)^{38}K^m$ reactions, with an energy standard based on $\alpha$ particles from radioactive sources. The present work used solid targets of $^{38}$Ar, isotopically enriched to 95%, in conjunction with the HISS system for energy determination, and aimed at a precision approaching 100 eV for the $^{38}\mathrm{Ar}(p,n)^{38}K^m$ threshold energy.

## II. METHOD

### A. Energy calibration

The Auckland heavy ion source system (HISS) has been described in some detail in Ref. [9], and its application to

 © 1998 The American Physical Society

determining the $^{26}Al^m$ and $^{34}Cl$ superallowed positron decay $Q$ values may be found in Refs [4,5]. Briefly, the proton beam from the AURA2 tandem accelerator, with energy full width at half maximum (FWHM) of perhaps 300 ppm, passes on a tightly collimated path around an Enge split-pole spectrograph and emerges with an energy distribution which is closely Gaussian, and which is adjustable in FWHM from 50 to 200 ppm. The entrance angles of the beam are $\pm 0.13°$ horizontally and $\pm 0.47°$ vertically and there are essentially no aberration effects in the image formation.

After the beam emerges, it travels a further 500 mm where it impinges on the target of interest. At intervals during a nuclear physics experiment, the proton beam is interrupted upstream, and the magnetic rigidity of the spectrograph orbit is calibrated by accelerating a beam of $^{133}Cs^+$ ions, generated by surface ionization, from rest through a voltage difference $V$ so that they pursue the same path as the protons had done. The magnetic field is essentially unchanged and is monitored by an NMR probe. Since the energy distribution of the transmitted beam depends only on the geometry, a scan of transmitted ion beam intensity as a function of $V$ provides not only the energy details of the $^{133}Cs$ beam, but also those of the protons. The voltage $V$, which for the present measurements was around 53 kV, is measured by first dividing it by a fixed ratio of 10 001 in a passive network and then comparing that output with a 1 V standard using a variable seven-decade Kelvin-Varley divider. There are several small factors at the level of several tens of ppm which contribute to the determination of $V$ and these are discussed in detail in Refs [9,10]. Improvements to the system made since the reports in Refs [4,5] include a more efficient technique for absorbing the Cs atoms into the ionizing surface and this has enabled more frequent calibrations during nuclear physics experiments and checking of the 10 001 ratio in between. In addition, the introduction of a new, self-calibrating Kelvin-Varley divider has reduced uncertainties in the overall procedure. Overall, a single HISS calibration will normally establish a proton energy to $\sim 15$ ppm, and this is reduced to $\sim 10$ ppm by taking several calibrations over the course of a day.

### B. Threshold measurement

After exiting the spectrograph, the proton beam entered the $^{38}Ar$ target chamber. This was cylindrical with the axis perpendicular to the beam and about 375 mm long, and a diameter of 90 mm. Along the axis was a cold leg coming down from the second stage of a Gifford-McMahon helium refrigerator, and a copper cold foot, whose temperature was normally between 8 and 12 K, sat just above the proton beam axis. The whole of the low-temperature surface was surrounded by a silver heat shield at 80 K, to lower the radiative heat load, and the vacuum was maintained by a small turbomolecular pump. Base pressures were around $10^{-8}$ Torr when the system was isolated and at room temperature, and somewhat higher when it was open to the spectrograph vacuum system. On the cold foot was a substrate of 99.995% pure gold, 0.125 mm thick, and targets of $^{38}Ar$ were made by squirting a small, calibrated amount of gas at this gold. The yield of $^{38}K^m$ was monitored by detecting the positrons (maximum energy 5 MeV) from its decay back down to $^{38}Ar$. The number of protons striking the target was monitored by detecting protons scattered from the target at roughly 135° into a silicon semiconductor detector. The heat shield therefore had three circular holes, 15 mm diameter, in it: the entrance for the protons, the exit for the backscattered protons, and the aperture for the argon gas pipe. In addition, in order to reduce the energy degradation of the exiting positrons, a 30 mm diameter circle was cut out of the heat shield behind the target and replaced by a 0.125 mm thick copper foil.

The positrons were detected in a three component, $\Delta E$-$\Delta E$-$E$ telescope of which the first two elements were 28 mm square, 300 $\mu$m thick silicon PIN transmission diodes and the third a 25 mm square CsI(Tl) crystal, 10 mm thick, optically coupled to a similar diode. To be counted, a $^{38}K^m$ positron had first to pass through the 0.125 mm gold substrate, the 0.125 mm copper heat shield and a 0.075 mm stainless steel vacuum seal. It then was required to trigger a 0.5 $\mu$s coincidence in the first two detectors, and produce an energy pulse in the third. With the data rates encountered, random coincidence rates were negligibly small, but the arrangement described minimized the occurrence of true events triggered by $\gamma$ rays. The distance from the $^{38}Ar$ target to the CsI crystal was 30 mm.

Extensive testing was devoted to answering the questions: ''What proportion of the gaseous argon froze on impact?'' and ''How much power, or power density, could the target absorb before the argon started to boil off?'' For the former, a target of aluminum, approximately 20 keV thick to a 7 MeV proton beam, was evaporated on to a 99.995% pure gold substrate and placed in the target position on the cold foot. A yield curve of the $^{27}Si$ positrons from the $^{27}Al(p,n)^{27}Si$ reaction was then taken in the region of threshold, and the threshold energy established. A calibrated amount (in $cm^3$ in Hg) of natural argon (not $^{38}Ar$) was then squirted on the cold foot and the consequent movement of the threshold energy determined. This was repeated several times, and the energy shifts converted to argon areal densities using standard energy loss tables. The conclusion was that ''perhaps half'' of the argon froze but, more importantly, that the correspondence between amount of input gas and thickness of solid target produced was reproducible.

To answer the second question, a target of frozen, natural argon, approximately 10 keV thick, was bombarded with a beam of 7 MeV protons, and the yield of 1459 keV $\gamma$ rays from the reaction $^{40}Ar(p,p')$ was monitored as a function of beam intensity, using a germanium detector. It was found fairly consistently that no diminution of yield occurred for beam currents of less than 130 nA, but that by 150 nA the target was starting to evaporate, and this was despite the fact that the temperature indicated by the thermometer attached to the cold foot did not rise above 16 K. The limiting factor was most probably the thermal conductivity of the 0.125 mm thick gold foil. This test drove us to limit the beam current in the actual $^{38}Ar$ runs to 80 nA.

There were ten measurements of the $^{38}Ar(p,n)^{38}K^m$ yield curve, each with a fresh target. Each was taken as approximately 20 yield points within 4 keV of the threshold energy, i.e., from 7004 to 7012 keV proton energy. At a particular proton energy, the target was bombarded for a fixed time, either 2 or 3 seconds, and the total number of backscattered

protons recorded. The beam was then interrupted 5 m upstream of the spectrograph, behind a shielding wall, with a magnetic deflector, and the positron spectrum recorded for the same time. This beam-on/beam-off cycle was repeated either 300 or 200 times, after which the proton beam energy was changed by altering slightly the spectrograph field and its NMR frequency (typically by $\sim 0.02\%$) and the process repeated. Investigation of the possibility of systematic error being introduced into the energy calibration by field changes of this magnitude is incorporated automatically into the prerun and postrun measurements of the $X$ value, which are performed over a wider range of field variations than are the actual proton runs. No effect has ever been seen, down to the level of a few ppm. This is entirely in accord with the overall behavior of the HISS system, in which the maximum differential hysteresis measured, as reflected in the $X$ values for the magnetic fields for 1 and 7 MeV, is 140 ppm.

The positron data were taken in event-mode form with two parameters, the first being the gated energy signal and the second being the time after the start of the beam-off cycle at which the positron was detected. The organization of the data taking and beam cycling was made using a Camac system. To monitor the state of the $^{38}$Ar target, $\gamma$-ray spectra were accumulated during the beam-on periods and the yield of the 1.21 MeV $\gamma$ ray from the decay of the $^{38}$Ar second excited state was observed. Unfortunately, this yield was not very large and so the test was not as sensitive as desired. The $\gamma$ ray from the first excited state could not be used because it was also produced plentifully following the positron decay of $^{38}$K, with halflife 7 min. No evidence was seen in any of the runs that the target was evaporating.

During the day prior to the acquisition of a yield curve, several HISS calibrations of the magnetic rigidity $X$ (strictly speaking a factor proportional to the square of the mean radius, in units of u eV MHz$^{-2}$) of the central spectrograph orbit were made, and the average value was then used to calculate the proton kinetic energies for the following yield points. After a yield curve had been finished, several more calibrations were made and the proton energies slightly revised (by a few ppm) in light of the overall average.

## III. RESULTS

In the analysis of the event-mode data, it had originally been intended to project the positron yield data on to the time axis, using various cuts on the energy axis. The time data was then to be analyzed to find the amplitude of the component which decayed with the identifying halflife of $^{38}K^m$, 0.92 s, and this was expected to produce very good yield to background ratios and a high quality yield curve. Unfortunately another factor intervened. Figure 1 shows projected positron spectra at proton energies 4 keV below and 4 keV above the $^{38}K^m$ threshold, from run 10. The continuum ending at approximately 3.3 MeV is not from a contaminant in the target, but rather from the 7 min activity of $^{38}$K produced from the target material itself. The yield of this is large because the proton energy is 130 keV above the threshold for its production. Although a 7 min activity is essentially flat in a 2 or 3 sec time projection, the statistical fluctuations in the time channel contents swamp the small signal from the $^{38}K^m$, and so the analysis had to be restricted to positron

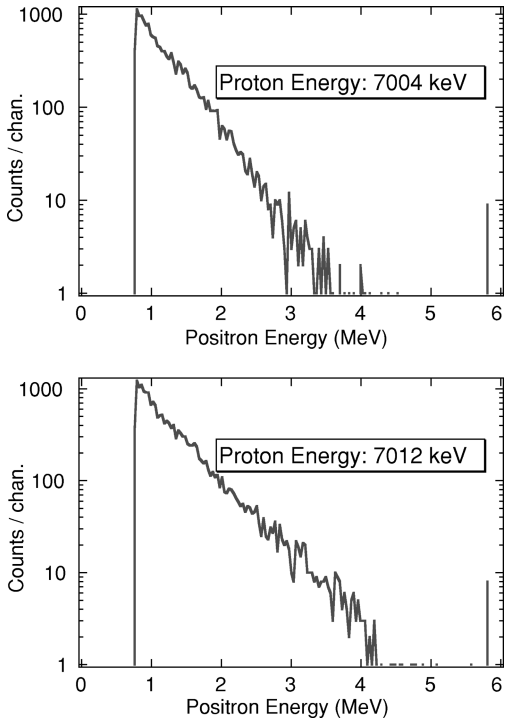


FIG. 1. Positron energy spectra during beam-off periods, from the reaction of proton beams of energies 7004 and 7012 keV with a target of frozen $^{38}$Ar.

energies greater than the $^{38}$K end point. However, even this is not clear cut, since the $^{38}$K positron energy can be augmented either by the 1.46 MeV $\gamma$ ray which is emitted simultaneously and which may enter the CsI detector, or by one of the 511 keV $\gamma$ rays produced in the CsI detector when the positron annihilates there. After much examination of the data, it was decided that the cleanest and most unambiguous signal of the yield was provided by a simple projection on to the energy axis, and the integration of an energy cut from 2.7 to 4.5 MeV. Energy cuts with lower limits ranging from 2.1 to 3.5 MeV were investigated, and found to give thresholds in agreement with the results presented, but with larger uncertainties.

In Fig. 2 is shown the yield curve for run 10. The error

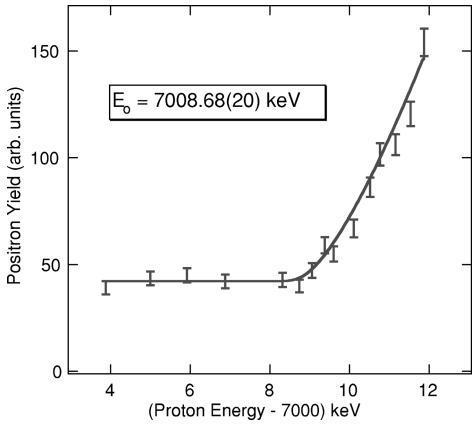


FIG. 2. The yield curve from run 10 of positrons following the reaction $^{38}$Ar$(p,n)^{38}K^m$. The points are the experimental data, the continuous line is the fit to the data to extract the threshold energy $E_0$, as discussed in the text.

bars represent the Poisson fluctuations in the positron yields outlined above. The straightforward way to extract the threshold energy $E_0$ from the data is to assume that the neutron emission in the $(p,n)$ reaction a few keV above $E_0$ is $s$ wave and therefore the cross-section depends on the proton energy $E$ as $(E\text{-}E_0)^{1/2}$. On the further assumption that the protons lose energy uniformly in the argon target, the thick target yield becomes proportional to $(E\text{-}E_0)^{3/2}$, where ''thick target'' means that the proton energy falls below $E_0$ before it exits the back of the target. So a yield curve is analyzed by fitting the data to the function $y=\alpha_1+\alpha_2(E\text{-}E_0)^{3/2}$, and the threshold energy is extracted.

There are, however, four features which are omitted from this treatment but which are not negligible at the level of accuracy hoped for. Three of them have been discussed in detail in Ref. [4] and by Amundsen and Barker [11] and will be described only briefly here. First, the proton beam is not monoenergetic, but its energy is Gaussian distributed with a known FWHM. Secondly, the protons do not lose energy uniformly, but rather undergo losses in which the probability of losing energy $Q$ is proportional to $1/Q^2$, which means that a ''snapshot'' at any instant of the energy profile of the protons in the target would show more higher energy particles than predicted by the assumption of uniformity. Thirdly, some protons during the reactions which produce $^{38}K^m$ nuclei will also ionize the atoms, and so will require more energy. Calculations of the differential probabilities for ionization of the argon subshells have been made, as we described previously in Ref. [11].

Up to now, the attitude to incorporation of the above effects has been to analyze yield curves simply according to the $(E\text{-}E_0)^{3/2}$ dependency, and then to apply three ''corrections,'' $\Delta_{\text{Gauss}}$, $\Delta_Q$, and $\Delta_{\text{ion}}$ to the extracted $E_0$ (see, e.g., Ref. [5]). Although this is not inadequate, it is obviously inferior to fitting the data to a yield function which contains the effects *a priori*, and the latter approach has been taken in the present work. Accordingly, an $(E\text{-}E_0)^{1/2}$ yield set was created in 1 eV steps and then convolved with a $1/Q^2$ energy loss distribution which had been calculated by a Monte Carlo technique. The result was further convolved with a Gaussian beam energy spread, with widths in the present case of 85 or 130 ppm, and this was finally convolved sequentially with the differential energy loss probability functions for ionization of the $K$, $L1$, $L2$, $L3$, $M1$, $M2$, and $M3$ argon subshells, to produce a yield function in the form of a look-up table in 1 eV steps, $Y_{\text{look}}(E,E_0)$.

The fourth factor influencing the analysis at the 100 eV level is particular to low-temperature experiments such as ours. At a base pressure of $10^{-8}$ Torr, assumed due mainly to nitrogen gas at room temperature, the target is subjected to $4\times10^{12}$ collisions/(cm$^2$ s) by gas molecules. If all these molecules stick, a layer builds up on the front of the argon at a rate corresponding to 35 eV/hour for a 7 MeV proton beam, and the loss of this energy by the protons before they strike the argon is reflected in the $^{38}K^m$ yield curve. This effect was investigated during a preliminary yield curve by returning five times at roughly 2.5 h intervals to a yield point using a proton beam energy of 7011 keV. The rate of accretion was found to be quite constant and at that stage was 270 eV/h, which was in reasonable accord with the pressure which had been indicated on the system vacuum gauge before cooling had started. Between runs 3 and 4 the vacuum was markedly improved by removing a defective flange and the pressure fell then to $10^{-8}$ Torr, the consequence of which may be seen in Table I. In the analysis of yield curves, this effect was dealt with by using as the proton energy not $E$, but rather $(E\text{-}\alpha_3 t)$, where $\alpha_3$ is the rate of accretion, in eV/h, and $t$ is the time which has elapsed since the manufacture of the target.

TABLE I. Summary of the results for the 10 yield curves described in the text. Shown for each are the beam energy FWHM, the calibration $X$ number, the extracted accretion rate and threshold energy, and the normalized chi-square for the fit. Runs 1 and 2 had the $X$ value in common, as did runs 3 and 4, and runs 5, 6, and 7.

| Run | Beam FWHM (eV) | $X$ (u eV MHz$^{-2}$) | Accretion (eV/h) | $(E_0-7000)$ (keV) | $\chi^2_\nu$ |
|---|---|---|---|---|---|
| 1 | 910 | 7770.09(11) | 99(28) | 8.87(19) | 2.2 |
| 2 | 910 | 7770.09(11) | 201(87) | 7.79(53) | 3.3 |
| 3 | 910 | 7770.03(12) | 145(54) | 8.34(37) | 2.8 |
| 4 | 910 | 7770.03(12) | 46(17) | 8.17(18) | 1.9 |
| 5 | 910 | 7770.05(14) | 29(19) | 8.57(15) | 1.2 |
| 6 | 910 | 7770.05(14) | 12(25) | 8.71(22) | 2.2 |
| 7 | 910 | 7770.05(14) | 16(20) | 8.28(20) | 1.2 |
| 8 | 600 | 7769.84(8) | 53(21) | 8.57(15) | 2.2 |
| 9 | 600 | 7770.96(8) | 42(37) | 8.63(34) | 2.9 |
| 10 | 600 | 7769.08(8) | 26(24) | 8.68(20) | 1.3 |

An experimental yield curve was then fitted in a normal, nonlinear least squares way to a form $Y=\alpha_1 Y_{\text{look}}(E\text{-}\alpha_3 t,E_0)+\alpha_2$ and the constants $\alpha_1$, $\alpha_2$, and $\alpha_3$, and the threshold energy $E_0$ extracted. Such a fitted yield for run 10 is shown in Fig. 2, where the abscissa is actually the proton energy $(E\text{-}\alpha_3 t)$, and the normalized chi-square for the fit is 1.2.

In Table I are shown the results of the analyses of the 10 runs. The $X$ calibration values are included to give an indication of the errors introduced by that part of the procedure. To give an indication of the magnitudes of the three corrections discussed above, $\Delta_{\text{Gauss}}$, $\Delta_Q$, and $\Delta_{\text{ion}}$ would have been $+0.04$ or $+0.02$ keV (for the 130 or 85 ppm FWHM), $+0.19$ and $-0.07$ keV, respectively (although they were not actually applied as external corrections, as explained). The accretion rate $\alpha_3$ may be seen in the table. The errors on the quoted threshold values are solely those from the fitting of the yield curves, as discussed above, and they reflect the normalized chi-square values given in the table.

Some of the earlier runs had $X$ values in common, and this was taken into account in the derivation of the overall average threshold energy, and of its associated error. For instance, the $E_0$ values from runs 1 and 2 were averaged together to give 7008.75(34) keV and then the error from their joint $X$ calibration folded in to give 7008.75(36) keV. This procedure applied throughout gave six independent values for $E_0$ whose average was 7008.52(9) keV. Incorporating an 8 ppm systematic error in the HISS calibration procedure and a further 55 and 25 eV for the uncertainties in $\Delta_Q$ and $\Delta_{\text{ion}}$ leads to a final threshold value of 7008.52(12) keV.

The threshold energy in the laboratory frame must be converted (relativistically) into a $Q$ value in the center of mass frame, and the question arises as to whether the recoiling

mass should be treated as an atom or as a nucleus. In the present case, and as emphasized in Ref. [11], the ionization energy loss probability calculations referred to above specifically include the recoil correction, and the mass which must be used is that of the atom. This gives a final value for $Q_{ec}$, the ''electron capture'' $Q$ value of $^{38}K^m$, of 6044.37(12) keV, where 782.354 keV has been used for the mass difference of the neutron and the hydrogen atom.

This value is in good agreement with, but is more precise than, the three values cited in the Introduction. A weighted average of all four is 6044.34(12) keV. Accepting this mean to replace that in Ref. [1] improves the calculated $f$ value from 3295.9(17) to 3297.7(4). This then improves the ft value quoted in Ref. [2] from 3047.9(26) s to 3049.4(21) s, and the ft value, which includes the theoretical corrections $\delta_R = 1.33(4)\%$ and $\delta_C = 0.62(3)\%$, is moved from 3069.4(31) s to 3070.9(27) s.

## IV. CONCLUSIONS

The precision of our knowledge of the energy release of the superallowed beta decay of $^{38}K^m$ has been improved by nearly a factor 5, so that the proportional error in the $f$ value is now 0.012%. However, the error in the ft value is still 0.088%. This is because the contribution to ft from the halflife value is 0.068% and that from the theory calculations of the corrections is 0.055%. From an experimental point of view, our knowledge of the halflife should be improved so that the uncertainties in the theoretical calculations can be isolated, and hopefully reduced.

There are five measurements of the halflife of $^{38}K^m$ cited in Ref. [1]: 925.5(7), 922.3(11), 921.71(65), 928.8(20), and 924.15(31) ms. In this reference, the weighted mean of these obviously discrepant values is given a confidence level of 0%, and so to take this into account, the errors are inflated, in this case by a factor 2.6. This is a fairly standard procedure, but it makes the data set very hard to influence if all the values are retained. Another measurement, equal in precision to the best of the set, can do no better than reduce the ascribed error from 0.64 to 0.45 ms. To do better than this would indeed be a challenge.

## ACKNOWLEDGMENTS

As always, the authors would like to acknowledge the dedicated support of the technical staff of the AURA2 tandem accelerator laboratory, M. J. Keeling and W. B. Wood. In addition, we would like to warmly thank Professor Sharpey-Shafer, until recently of the Daresbury tandem accelerator laboratory and Liverpool University, for the gift of exactly the right amount of enriched $^{38}Ar$ gas.

[1] J. C. Hardy, I. S. Towner, V. T. Koslowsky, E. Hagberg, and H. Schmeing, Nucl. Phys. **A509**, 429 (1990).

[2] I. S. Towner, E. Hagberg, J. C. Hardy, V. T. Koslowsky, and G. Savard, in *Proceedings of the International Conference on Exotic Nuclei and Atomic Masses*, Arles, France, 1995, edited by M. de Saint Simon and O. Sorlin (Editions Frontières, Gif-sur-Yvette, 1995), p. 711.

[3] I. S. Towner and J. C. Hardy, *Symmetries and Fundamental Interactions in Nuclei*, edited by W. C. Haxton and E. M. Henley (World Scientific, Singapore, 1995).

[4] S. Lin, S. A. Brindhaban, and P. H. Barker, Phys. Rev. C **49**, 3098 (1994).

[5] S. A. Brindhaban and P. H. Barker, Phys. Rev. C **49**, 2401 (1994).

[6] G. T. A. Squier, W. E. Burcham, J. M. Freeman, R. J. Petty, S. D. Hoath, and J. S. Ryder, Nucl. Phys. **A242**, 62 (1975).

[7] A. N. James, J.-F. Sharpey-Shafer, A. M. Al-Naser, A. H. Behbehani, C. J. Lister, P. J. Nolan, P. H. Barker, and W. E. Burcham, J. Phys. G **4**, 579 (1978).

[8] W. E. Burcham, G. T. A. Squier, P. H. Barker, J. M. Freeman, and S. D. Hoath, Nucl. Instrum. Methods **164**, 533 (1979).

[9] S. A. Brindhaban, P. H. Barker, M. J. Keeling, and W. B. Wood, Nucl. Instrum. Methods Phys. Res. A **340**, 436 (1994).

[10] P. H. Barker, S. C. Baker, S. A. Brindhaban, and M. J. Brown, Nucl. Instrum. Methods Phys. Res. A **306**, 272 (1991).

[11] P. A. Amundsen and P. H. Barker, Phys. Rev. C **50**, 2466 (1994).